ELSEVIER

Bioelectrochemistry 55 (2002) 177–181

Bioelectrochemistry

www.elsevier.com/locate/bioelechem

Short communication

STM study of morphology and electron transport features in cytochrome *c* and nanocluster molecule monolayers

G.B. Khomutov [a,*], L.V. Belovolova [b], S.P. Gubin [c], V.V. Khanin [a], A.Yu. Obydenov [a], A.N. Sergeev-Cherenkov [a], E.S. Soldatov [a], A.S. Trifonov [a]

[a] *Faculty of Physics, Moscow State University, Vorobjevy Gory, 119899 Moscow, Russia*
[b] *General Physics Institute RAS, 119899 Moscow, Russia*
[c] *Institute of General and Inorganic Chemistry RAS, Moscow, Russia*

Received 1 June 2001; received in revised form 9 October 2001; accepted 15 October 2001

Abstract

The morphology and electron tunneling through single cytochrome *c* and nanocluster $Pt_5(CO)_7[P(C_6H_5)]_4$ molecules organized as monolayer Langmuir–Blodgett (LB) films on graphite substrate have been studied experimentally using scanning tunneling microscopy (STM) and spectroscopy techniques with sub-nanometer spatial resolution in a double barrier tunnel junction configuration STM tip–monomolecular film–conducting substrate at ambient conditions. STM images of the films revealed globular structures with characteristic diameters ($\sim$3.5 nm for the protein molecule and $\sim$1.2 nm for the nanocluster). The spectroscopic study by recording the tunneling current–bias voltage (I–V) curves revealed tunneling I–V characteristics with features as steps of different width and heights that are dependent on the STM tip position over the molecule in the monolayer, giving evidence for sequential discrete electron-tunneling effects with the combination of the single electron Coulomb-charging energy and the electronic energy level separation (molecular spectrum) in such immobilized metalloprotein and nanocluster structures that can be of interest for the development of bioelectronic and hybrid functional nanosystems.

Keywords: Cytochrome *c*; Nanocluster; Monolayer; Langmuir–Blodgett film; Electron transport; Electron tunneling; STM; Nanoelectronics

1. Introduction

The control of electron current at the level of single electrons is a challenge in nanoelectronics with the potential for the creation of circuits with extremely low dimensions and energy dissipation. Physical limitations for three-terminal nanoelectronic devices are concerned with the wave behavior of an electron at small device dimensions and problems with the determination of the electrochemical potential of tunneling electrons due to Heisenberg's uncertainty principle. Such limitations can be circumvented in a system where a number (at least two) of tunnel junctions were incorporated in the device with the sequential localized discrete character of electron transfer between the electrodes. In biological systems, the electron transfer processes are principal components of the stepwise oxidation–reduction reactions in electron transport chains in the membranes of the mitochondria (metabolic reduction of dioxygen), chloroplasts and bacteria (photoinduced electron transport). The importance of tunneling mechanism for biological redox electron transfer is due to the rather fixed and localized site nature of electron transfer in metalloproteins [1–3]. Thus, nature gives an example of the realization of multi-junction tunnel electronic system where electron current through a single molecule can be potentially controlled at the level of a single electron at ambient temperature.

Earlier in our group, we have introduced a bioinspired approach to create reproducible stable planar supramolecular structures based on the formation of biomimetic mixed Langmuir–Blodgett (LB) films consisting of inert amphiphile molecular matrix and guest chemically synthesized nanocluster molecules. Such nanostructures can serve as a model for the investigations of basic mechanisms of membrane redox reactions and are perspective for the development of room-temperature controlled single-electron tunneling molecular elements and systems [4]. The double tunnel junction (DTJ) structure "graphite substrate–nanocluster molecule–scanning tunneling microscope (STM)

* Corresponding author. Tel.: +7-95-939-3007; fax: +7-95-939-1195.
E-mail address: GBK@phys.msu.su (G.B. Khomutov).

1567-5394/02/$ - see front matter
PII: S1567-5394(01)00135-9

tip" was studied [5], and the effects related to single electron tunneling and discrete electronic level spectrum were observed in such structures at room temperature by STM [6]. Using such an approach, a single-electron tunneling transistor (SET) based on a single nanocluster molecule was demonstrated at room temperature for the first time [6,7].

STM allows to visualize the molecular nanostructures and study redox processes in the single molecules with high spatial and spectral resolution at ambient conditions [8,9]. The application of such technique to investigate the electrochemical electron transfer processes in single biological electron carriers such as metalloproteins with nanometer resolution is a new approach in nanobioelectrochemistry. The molecular structure of the samples for the investigations of single redox centers by this technique has to be the monolayer on the conducting substrate. Recently, immobilized protein monolayers were investigated by STM [10–12]. In the present work, we have used such an approach to study the electron transport features in the organized monomolecular films of cytochrome *c*—a protein electron carrier in the natural electron transport chains of the mitochondria. Cytochrome *c* is a well-characterized heme protein with a heme–iron redox center that has two redox levels accessible under physiological conditions, the oxidized (3+) and reduced (2+) levels. Cytochrome *c* is rather small protein (MW = 12 000) with a roughly spherical shape of 3.5 nm diameter. In this report, we present experimental results on the STM characterization of cytochrome *c* and the nanocluster $Pt_5(CO)_7[P(C_6H_5)_3]_4$ monolayer LB films on graphite substrates. The obtained experimental data on the STM study of the morphology and electron transport features in cytochrome *c* and the nanocluster molecular monolayers give evidence for close discrete electron-tunneling effects in such immobilized molecular structures.

2. Experimental

Cytochrome *c* (horse heart, MW = 12 000) was purchased from Sigma. Nanocluster molecules $Pt_5(CO)_7[P(C_6H_5)_3]_4$ used in the work were synthesized by Prof. S.P. Gubin in accordance with known procedures [13]. Such clusters have a metal nucleus surrounded by an organic shell which provides stability and atomic reproducibility of the nanocluster structure and tunnel barrier parameters. The last is of principal importance for the development of quantum devices, thus making nanoclusters prospective building blocks for the construction of nanoelectronic devices using self-organization and self-assembly principles. Water was purified by a Milli-Q system (Millipore). Monolayer cytochrome *c* Langmuir–Blodgett (LB) films on graphite substrates were prepared by preliminary solubilization of the protein in water bubbles of reverse microemulsion formed by anionic surfactant Aerosol OT (AOT) in hexane, protein/AOT complex Langmuir monolayer formation by spreading the microemulsion on the aqueous surface, monolayer compression and deposition [14]. The cytochrome *c*/AOT complex monolayer was transferred to a solid graphite substrate by a horizontal lifting method at the surface pressure value of 20 mN/m. Highly oriented pyrolytic graphite (HOPG) was used as the substrate to deposit monolayer films for investigations by STM. Surface pressure–monolayer area (p–A) isotherm measurements and monolayer transfer to solid substrates were carried out on a fully automatic conventional Teflon trough at 18–20 °C as described elsewhere [4]. Nanocluster Langmuir monolayers were formed by spreading a chloroform solution of nanoclusters or their mixtures with stearic acid (SA) (2×10^{-4} M) on the surface of purified water (pH = 5.9). After complete solvent evaporation, the floating monolayers were compressed by a mobile Teflon barrier at a speed of ~ 3 Å^2/molecule min and then deposited onto the HOPG substrate at a constant surface pressure (19–21 mN/m), temperature and substrate dipping speed using the conventional horizontal lifting method with good transfer ratios.

STM microtopographic images were obtained by recording the tip height at a constant tunnel current in a modified Nanoscop STM device (Digital Instruments) at an ambient temperature (21 °C); tunnel current $I = 0.2$ nA, and a bias voltage $V_{bias} = 200$ mV. The images were stable and reproducible. Single nanocluster and protein molecules were studied spectroscopically by recording tunnelling current–bias voltage (I–V) curves in a double barrier tunnel junction geometry at 21 °C, where the molecule was coupled via two tunnel junctions to the two macroscopic electrodes (HOPG substrate and the tip of the STM device).

3. Results and discussion

Fig. 1 shows STM topographic images of $Pt_5(CO)_7[P(C_6H_5)_3]_4$ (picture (a)) and cytochrome *c*/AOT complex monolayers (pictures (b) and (c)) deposited by the horizontal lifting method onto the surface of the HOPG substrate. The STM images of the monolayers were reproducible and revealed globular structures with characteristic diameters of ~ 12 Å for the nanocluster and about 3.5 nm for the protein corresponding to the geometries of these molecules known from the literature. The heights of cytochrome *c* molecules in Fig. 1 are smaller than that expected from the crystallographic data. Such effect is typical for the STM images of biomolecules where the heights measured by STM are systematically smaller than should be expected of them [15]. The reason for such effect can be connected with the specificity of the topographical measurements by STM, where the tunnel current (and thus, corresponding tunneling probability) is measured, that is not related directly to the dimensions of the real object. A submolecular structure with a central bright area is seen in the cytochrome *c* images, indicating the existence of a region with high tunneling probability in the central part of each cytochrome *c* molecule. Close fine features of brighter

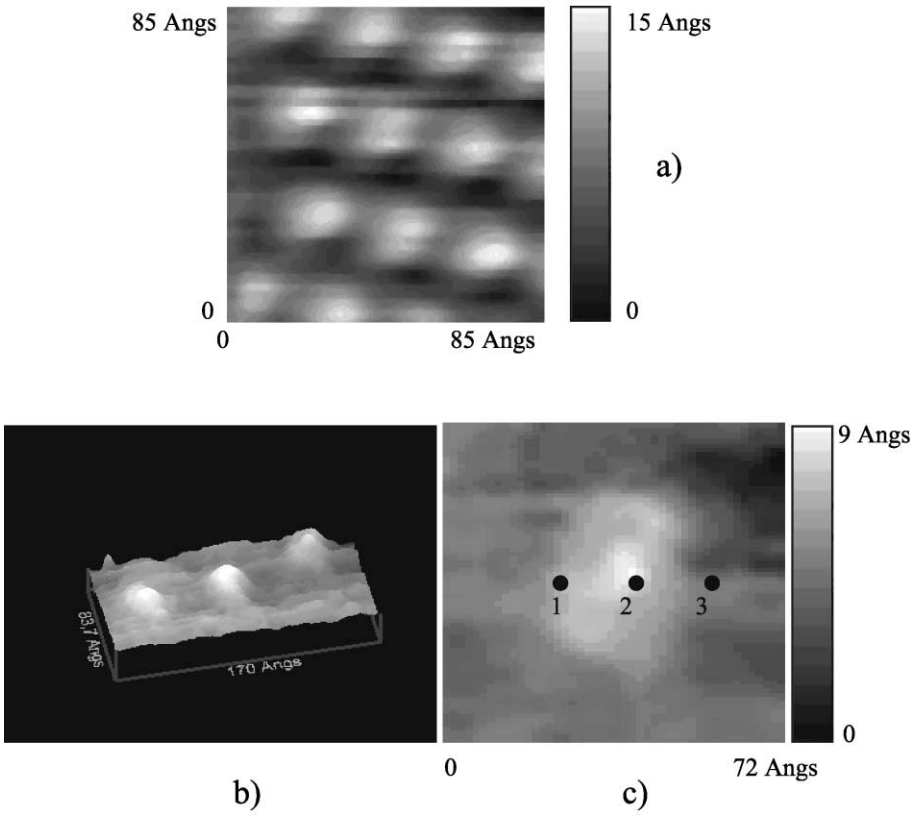

Fig. 1. STM topographic images of cytochrome *c*/AOT complex and $Pt_5(CO)_7[P(C_6H_5)_3]_4$ nanocluster monolayers deposited by the horizontal lifting method onto the surface of the highly oriented graphite substrate. (a) Top view image of the nanocluster monolayer (black to white vertical color scale is 0–1.5 nm); (b) 17×8.37 nm^2 3-D image (black to white vertical color scale is 0–1 nm) of a group of cytochrome *c* molecules; (c) 7.2×7.2 nm^2 top view image (black to white vertical color scale is 0–1 nm) of the individual cytochrome *c* molecule. Points 1–3 indicate the STM tip position over the protein molecule when the *I*–*V* curves were measured. Temperature: 21 °C.

contrast in the in situ STM image of the protein azurin on a gold substrate were reported in Ref. [16].

Typical *I*–*V* curves recorded at different STM tip positions over the cytochrome *c* molecule are shown on Fig. 2. Curves 1–3 correspond to the point numbers on Fig. 1(c). It can be seen from Fig. 2(a) that the shape of tunnel *I*–*V* curves depends substantially on the STM tip position point over the protein globule at which the electron tunneling was measured. Fig. 2(b) presents the spectroscopic d*I*/d*V* curve corresponding to curve 2 on Fig. 2(a) that was recorded over the center of the cytochrome *c* globule. The *I*–*V* curve over the center of a protein globule (curve 2 on Fig. 2(a)) is asymmetric and has a number of features ("steps" at 0.8, 1.3, −0.8 and −1.3 V). The *I*–*V* curves with similar features were recorded in a double tunnel junction configuration STM tip–nanocluster molecule–conducting substrate (the typical one is shown on Fig. 3). For comparison, the *I*–*V* curve obtained on the flat graphite substrate surface without protein or cluster molecules is presented on Fig. 3(b). Such symmetric smooth curves without the steps are typically observed for a single tunnel junction, which supports the fact that the rich structures in the *I*–*V* data are related to cytochrome *c* and nanocluster molecules. Asymmetric *I*–*V* curves were observed using STM in gold nanocluster tunnel systems at room temperature, and the existence of the background fractional charge Q_0 having an effect on the tunneling probability was proposed to explain an asymmetry of the *I*–*V* dependence [17]. The asymmetry of the *I*–*V* curves can also arise from the complex relations between the positioning of the Fermi level of the electrodes compared to the highest occupied molecular orbitals (HOMO) and the lowest unoccupied molecular orbitals (LUMO) in the neutral and ionized molecule. The conductivity contribution of the adsorbate, which may be present in the sample at ambient conditions, can also give rise to the *I*–*V* curve anisotropy. The complex rich structure of the tunneling current–voltage spectra obtained in the HOPG substrate/cytochrome *c* or nanocluster/STM tip system in our experiments is determined by the electron tunneling features in such system. If the resistance of the tunnel barriers in a double tunnel junctions system is much higher than the quantum unit of resistance R_Q ($h/e^2 \sim 26$ kΩ) due to long electron tunneling distances and high tunnel barriers, the electron transfer occurs in two independent sequential steps with the occupation and corresponding ionization of the central redox center. With this tunneling

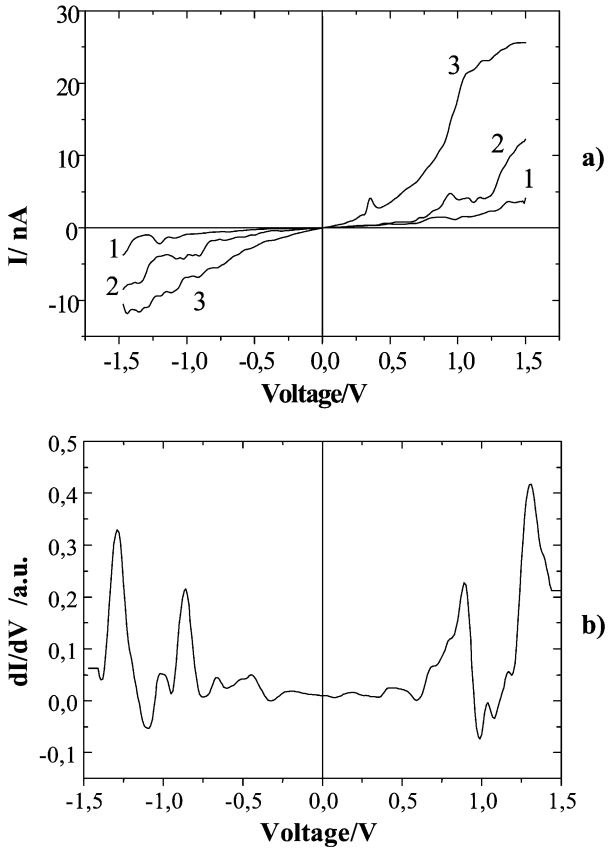

Fig. 2. STM tunneling current–voltage ($I-V$) characteristics in the double tunnel junction configuration STM tip–cytochrome *c* molecule–conducting HOPG substrate at 21 °C. (a) Characteristic $I-V$ curves recorded in different STM tip positions over the protein molecule (curves 1–3 correspond to the point numbers on Fig. 1(c). (b) Tunneling spectroscopic dI/dV curve corresponding to curve 2 on (a).

mechanism, the effects of single electron tunneling and energy quantization can be observed when the single electron Coulomb-charging energy and electronic level separation in the redox center exceed the thermal energy k_BT ($\sim$0.025 eV at 300 K) [18]. In our experiments, the resistance of the double junction system was of the order of $\sim 10^8$ Ω, which implies that the two-step sequential electron transfer between the electrodes via the cytochrome *c* molecule and nanocluster was realized. In this case, the complex features of electron tunneling in the graphite substrate/cytochrome *c* or nanocluster/STM tip system observed in our experiments resulted from both resonant tunneling through the discrete levels of cytochrome *c* and nanocluster molecules along with the charging effects. The experimentally measurable spectroscopic gap between the HOMO and the LUMO thus should be a combination of Coulomb blockade and the electronic energy level separation. An accurate theoretical fit to the experimental spectroscopic data presented in Figs. 2 and 3 is complicated by the dependence of the shape of the $I-V$ curves on both the tunnel junction parameters and the electronic molecular spectrum of the redox center in the concrete experimental conditions. The tunnel junctions parameters determine the value of the single electron-charging energy (that is dependent on the redox center effective capacity in the "orthodox" model of single electron tunneling [18]) and the values of parts of the total applied voltage which drop on each junction due to the division of applied voltage in the DTJ circuit. Those parameters have to be estimated independently from additional experiments or assumptions. The accurate attribution of each peak on the spectroscopic dI/dV curve corresponding to the resonant tunneling through a discrete redox center level also demands the information on the molecular level structure of the corresponding negatively or positively ionized redox center which is often hardly available.

The shape of the $I-V$ curves measured with the cytochrome *c* molecules can also reveal effects of specific "pathways" of the intramolecular electron transfer through the protein molecule when tunneling current is correspondingly dependent on the tip position over the molecule and on the molecule space orientation with respect to the substrate surface. This reflects the dependence of the anisotropic

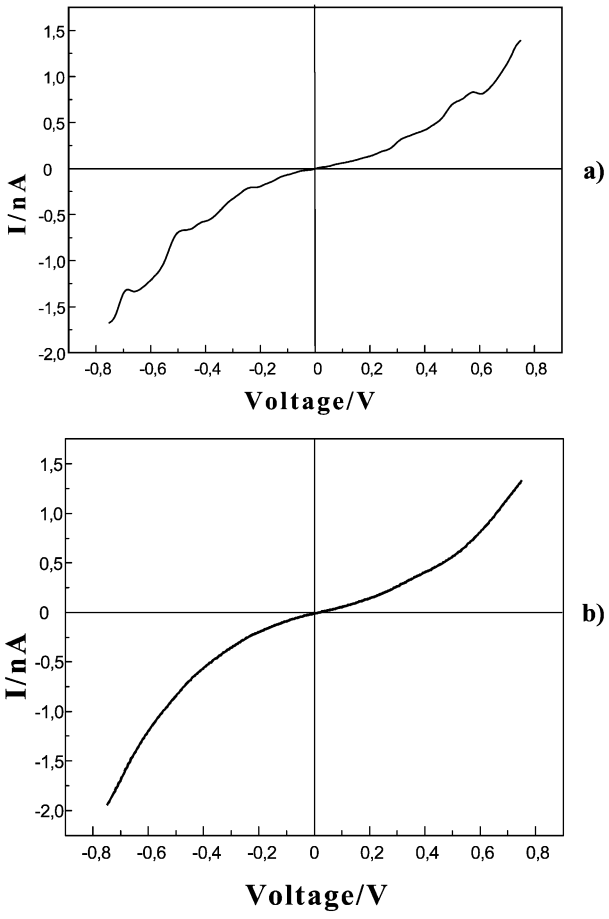

Fig. 3. STM tunneling current–voltage ($I-V$) characteristics in the double tunnel junction configuration STM tip–$Pt_5(CO)_7[P(C_6H_5)_3]_4$ nanocluster monolayer–conducting HOPG substrate at 21 °C. (a) Characteristic $I-V$ curve recorded over the nanocluster molecule. (b) Typical $I-V$ curve recorded on the flat HOPG substrate surface areas without the protein or nanocluster molecules.

electronic wave functions on the spatial location within the molecule, resulting in the corresponding dependencies of tunneling probability and the $I–V$ characteristics on the exact lateral tip position over the molecule. The conformational instability and reorganizations of the biomacromolecules under an electric field that is strong enough can also play an important role. The aforementioned circumstances at the moment make the detailed quantitative modeling of the obtained spectroscopic data a problem (it will be a subject of further research), but two resonances observed at applied voltage values below 1 V could be attributed to the physiologically important (3+/2+) redox reaction in the cytochrome *c* molecule.

Closely related effects of the discrete electron transport features observed in the metal–organic nanocluster LB monolayers give evidence for the closely similar nature of electron transport mechanisms in the nanocluster and cytochrome *c* nanostructures investigated in a double tunnel junction geometry. The analogy of the electron transport features in the immobilized nanocluster and cytochrome *c* systems allows us to assume the possibilities for the controllable compatible functioning of nanocluster-based nanoelectronic devices with biological and organic sensors and molecular microcircuits in hybrid electronic devices.

4. Conclusions

Monolayer LB films with cytochrome *c* and nanocluster molecules were deposited successfully on conducting HOPG substrate and were studied by the STM technique at ambient conditions. The high-resolution single molecule spectroscopic STM study was carried out by recording tunneling current–bias voltage ($I–V$) curves and non-symmetrical $I–V$ curves with the steps of variable widths and heights that were observed to be dependent on the point of the STM tip position over the protein molecule. The complex structure of the observed current–voltage characteristics can be due to the sequential discrete character of the electron transfer in the double tunnel junction configuration with the interplay between the Coulomb-charging effects and discreteness of the electronic spectrum of the molecule.

Acknowledgements

This work was supported by the Russian Foundation for Basic Researches (Grant 99-03-32218) and INTAS (Grant 99-864).

References

[1] A.M. Chang, R.H. Austin, Electron tunneling in cytochrome *c*, J. Chem. Phys. 77 (1982) 5272–5283.
[2] H. Sigel, A. Sigel (Eds.), Metal Ions in Biological Systems, vol. 27, Marcel Dekker, New York, 1991.
[3] D.S. Bendall (Ed.), Protein Electron Transfer, BIOS Publishers, Oxford, 1996.
[4] G.B. Khomutov, E.S. Soldatov, S.P. Gubin, S.A. Yakovenko, A.S. Trifonov, A.Yu. Obidenov, V.V. Khanin, Langmuir–Blodgett films in the development of high-temperature single electron tunneling devices, Thin Solid Films 327–329 (1998) 550–555.
[5] S.A. Yakovenko, E.S. Soldatov, V.V. Khanin, A.S. Trifonov, S.P. Gubin, G.B. Khomutov, Fabrication and properties of carborane clusters contained in stearic acid LB films and possible applications for single electron electronics, Thin Solid Films 284–285 (1996) 873–877.
[6] E.S. Soldatov, V.V. Khanin, A.S. Trifonov, S.P. Gubin, V.V. Kolesov, D.E. Presnov, S.A. Yakovenko, G.B. Khomutov, Single-electron transistor based on a single cluster molecule at room temperature, JETP Lett. 64 (1996) 556–561.
[7] S.P. Gubin, V.V. Kolesov, E.S. Soldatov, A.S. Trifonov, V.V. Khanin, G.B. Khomutov, S.A. Yakovenko, Tunneling device, US Patent 6,057,556, May 2, 2000.
[8] P.B. Lukins, Single-molecule electron tunneling spectroscopy of the higher plant light-harvesting complex LHCII, Biochem. Biophys. Res. Commun. 256 (1999) 288–295.
[9] D. Porath, Y. Levi, M. Tarabiah, O. Millo, Tunneling spectroscopy of isolated C_{60} molecules in the presence of charging effect, Phys. Rev. B 56 (1997) 9829–9835.
[10] M.E. Welland, M.J. Miles, N. Lambert, V.J. Morris, J.H. Coombs, J.B. Pethica, Structure of the globular protein vicilin revealed by scanning tunneling microscopy, Int. J. Biol. Macromol. 11 (1989) 29–36.
[11] J.E.T. Andersen, P. Moeler, M.V. Pedersen, J. Ulstrup, Cytochrome *c* dynamics at gold and glassy carbon surfaces monitored by in situ scanning tunnel microscopy, Surf. Sci. 325 (1995) 193–205.
[12] A. Tazi, S. Boussaad, J.A. DeRose, R.M. Leblanc, Structural investigation of cytochrome *f* Langmuir–Blodgett films with scanning tunneling microscopy: protein aggregation, J. Vac. Sci. Technol. B 14 (1996) 1476–1480.
[13] N.K. Eremenko, E.G. Mednikov, S.S. Kurasov, Carbonyl–phosphine clusters of Pd and Pt, Usp. Khim. LIV (1985) 671–695.
[14] L.V. Belovolova, T.V. Konforkina, V.V. Savransky, H. Lemmetyinen, Mono- and multilayer Langmuir films of cytochrome *c*–aerosol OT, Mol. Mater. 6 (1996) 189–197.
[15] R. Garcia, Comments on direct visualization of protein complexes by scanning tunneling microscopy, Biophys. J. 60 (1991) 738.
[16] P.E. Fris, J.E.T. Andersen, Yu.I. Kharkats, A.M. Kuznetsov, R.J. Nichols, J.-D. Zhang, J. Ulstrup, An approach to long-range electron transfer mechanisms in metalloproteins: in situ scanning tunneling microscopy with submolecular resolution, Proc. Natl. Acad. Sci. U. S. A. 96 (1999) 1379–1387.
[17] R.P. Andres, T. Bein, M. Dorogi, S. Feng, J.I. Henderson, C.P. Kubiak, W. Mahoney, R.G. Osifchin, R. Reifenberger, "Coulomb staircase" at room temperature in a self-assembled molecular nanostructure, Science 272 (1996) 1323–1328.
[18] K.K. Likharev, Single-electron devices and their applications, Proc. IEEE 87 (1999) 606–656.